



Original Paper

Static Reservoir Modeling of the Eocene Clastic Reservoirs in the Q-Field, Niger Delta, Nigeria

Austin E. Okoli,^{1,2} Okechukwu E. Agbasi^{3,6}, Aref A. Lashin,⁴ and Souvik Sen⁵

Received 15 October 2020; accepted 24 December 2020
Published online: 8 January 2021

This work integrates seismic and well log data to establish a 3D reservoir model of the Q-Field, which is a prolific onshore hydrocarbon field situated in the Central Swamp Depobelt of Nigeria. The subsurface modeling focuses on the four principal clastic reservoir intervals of the Agbada Formation (D6200, D7000, D9000 and E2000), which was deposited in a deltaic to fluvio-deltaic system during Eocene. The seismic-based structural modeling inferred an extensional set-up dominated by NW–SE trending normal faults. Reservoirs are sand-dominated and laterally extensive, as interpreted from the 3D facies model. Well log-based petrophysical parameters were up-scaled and distributed stochastically using the Sequential Gaussian Simulation method to generate a 3D reservoir property model. Lateral and vertical heterogeneities of the reservoir properties were inferred from the 3D models. In general, the clastic reservoirs exhibit 18–22% porosity, 62–105 mD permeability, moderate to good net-gross thickness, and 36–74% water saturation. Hydrocarbon accumulation was primarily restricted within the anticlines. Gas-down-to exists in the upper three reservoirs (D6200, D7000 and D9000) at 10,577 ft (1 ft = 0.3048 m), 10,756 ft and 11,389 ft, respectively. Gas–oil and oil–water contacts in the E2000 reservoir were interpreted to be at 11,812 ft and 11,886 ft, respectively. Based on the hydrocarbon distribution, oil and gas-in-place volumes were estimated for all the reservoir intervals. The comprehensive 3D modeling work addressed the spatial distribution of the studied reservoir properties and can be directly useful for planning better the future wells for field development.

KEY WORDS: Seismic interpretation, Structural modeling, Petrophysics, 3D reservoir modeling.

INTRODUCTION

Complexity of depositional environment, geological settings and heterogeneity of reservoir parameters result in intricacy of resource identification and prospect generation, which affect directly well production performance, success of field development and cost-effectiveness (Ma and Pointe 2011; Adeoti et al. 2014; Seyyedattar et al. 2020). A comprehensive 3D reservoir model is essential to address the spatial reservoir property distribution (Abdel-Fattah et al. 2018; Adesoji et al. 2018; Oyeyemi et al. 2018). It involves interpretation of necessary and available geological and geophysical

¹School of Engineering, Geosciences, Infrastructure and Society, Heriot Watt University, Edinburgh EH14 4AS, UK.

²Department of Geology, Federal University of Technology, Owerri, Imo State, Nigeria.

³Department of Physics, Michael Okpara University of Agriculture, Umudike, Abia State, Nigeria.

⁴Petroleum and Natural Gas Engineering Department, College of Engineering, King Saud University, P.O. Box 800 Riyadh 11421, Saudi Arabia.

⁵Geologix Limited, Dynasty Building, Andheri Kurla Road, Andheri (E), Mumbai 400059, Maharashtra, India.

⁶To whom correspondence should be addressed; e-mail: agbasi.okechukwu@gmail.com

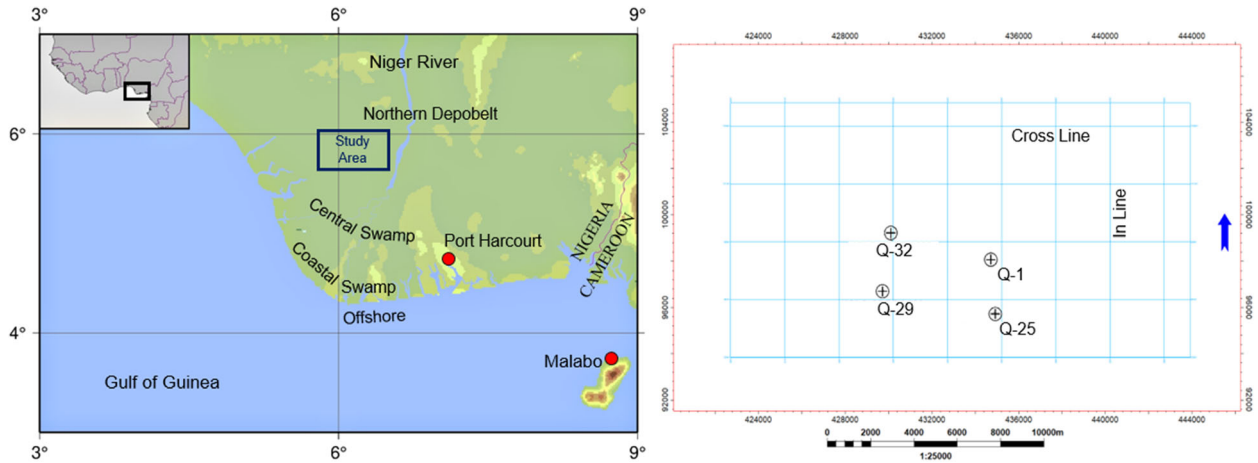


Figure 1. Location of the studied Q-Field in the Niger Delta (left). Base concession map showing seismic inline-crossline coverages and well locations (right).

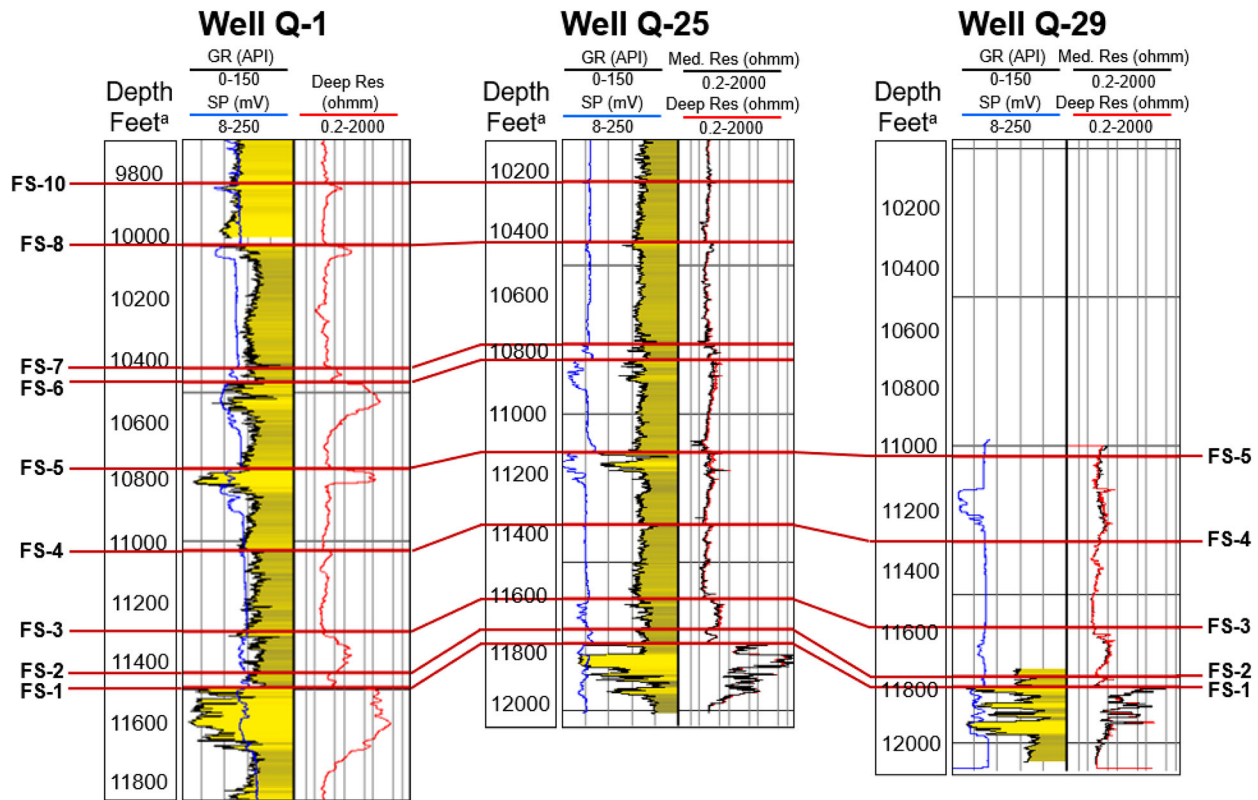


Figure 2. Well log correlations between the studied wells. 'FS' indicates the interpreted major flooding surfaces and correlated across the wells [1 ft = 0.3048 m].

data to characterize, among others, structural elements, facies architecture and critical petrophysical properties like porosity, permeability, net-to-gross

thickness and water saturation (Yu et al. 2011; Abdel-Fattah et al. 2018; Adelu et al. 2019). As drilling and field development progress, the initially built

reservoir models are updated with additional drilled well data, and further refinement as well as complexity in the geological interpretation is introduced (Abdel-Fattah et al. 2010). This work attempted to establish the first 3D static reservoir model of the Q-Field, situated in the Niger Delta, Nigeria. The Niger Delta is an established prolific petroleum system, with extensive hydrocarbon accumulation in the clastic sequences of the Eocene Agbada Formation.

Researchers have utilized subsurface modeling workflows to address fault geometry (Adagunodo et al. 2017; Adelu et al. 2019), facies analysis (Aigbadon et al. 2017; Jika et al. 2019), petrophysical analysis (Alao et al. 2013; Adiola 2018; Ndip et al. 2018; Farouk et al. 2017; Kalu et al. 2020), hydrocarbon prospectivity (Omoja and Obiekezie 2018), hydrocarbon volume estimation (Oluwadare et al. 2017; Okpogo et al. 2018), reservoir production history matching (Ahmed et al. 2011) from the various oil and gas fields in the Niger Delta. This work provides all these deliverables and presents a robust fit-for-purpose 3D reservoir model of the onshore Q-Field by integrating seismic data as well as wireline logs from drilled wells. The principal objectives of the work were: (1) to interpret faults from the seismic volume and prepare a structural model; (2) to interpret key petrophysical properties from well logs and populate those in the 3D reservoir model; (3) to assess the reservoir properties and their spatial distribution within the facies model at the D6200, D7000, D9000 and E2000 reservoir intervals by 3D reservoir petrophysical models; and (4) to analyze the hydrocarbon distribution, fluid

Table 1. Vintage seismic properties available in the studied Q-Field

Geometric properties	Values
Total coverage area	177 km ²
Co-ordinate reference system	Nigeria Mid Belt-Minna (NIGERIMB)
Inline range	8091–8939
Crossline range	93,481–93,841
Time slice range	0–600 ms
Bin size (m)	25 × 25
Sample interval	4 m
Dominant frequency	15 Hz

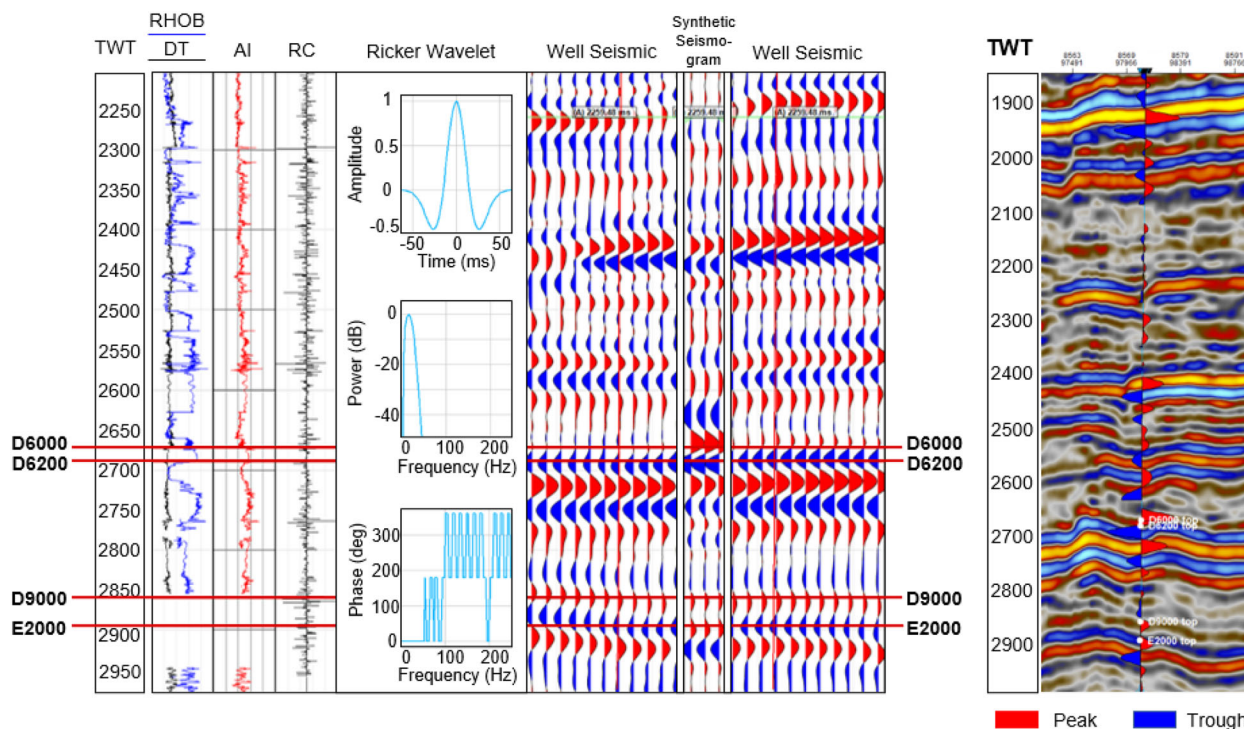


Figure 3. Well to seismic tie using the well Q-1 (post-tie). TWT is two-way time (ms). The second track plots density (RHOB) and sonic slowness (DT), which were combined to generate the acoustic impedance (AI on third track) and then reflection coefficients (RC on fourth track). RC and Ricker wavelets were integrated to generate synthetic seismogram, which was then tied back to seismic data by adjusting a bulk shift.

contact levels and estimate the hydrocarbon-in-place volumes based on the initial modeling results.

GEOLOGY OF THE STUDY AREA

The Niger Delta Basin is a large rift basin located on the reactive continental margin near Nigeria’s west coast, mainly in the Niger Delta and the Gulf of Guinea, with suspected or confirmed access to Cameroon, Equatorial Guinea and São Tomé and Príncipe (Agbasi et al. 2018, 2020). The Niger Delta Basin lies within a wider tectonic structure in the south-westernmost part, situated within 4°–9°E longitude and 4°–9°N latitude. This basin is very complex and has high economic value because it contains a proven petroleum system, hosted by more than 25,000 ft (1 ft = 0.3048 m) of sedimentary column, affected by regional tectonics (Inyang et al. 2018). The vast Niger Delta Basin is flanked by other basins in the offset region, influenced by similar structural evolution. The studied Q-Field is situated in the onshore central swamp depobelt region. Figure 1 presents a generalized location map of the study area, along with the base concession map with the available seismic inline-crosslines and studied well locations. The extraordinarily thick sedimentary succession is characterized by three principal lithofacies: (a) thick shales of the Akata Formation at the bottom; (b) marginal marine clastics of the Agbada Formation; and (c) extensive coastal sandstones of the Benin Formation. The Paleocene Akata Formation is characterized by marine shales with source rock qualities, and in the central part of the delta, its maximum thickness reaches up to 20,000 ft. The Eocene Agbada Formation is the principal hydrocarbon-bearing unit, which was deposited in a deltaic to fluvio-deltaic system (Ejedavwe et al. 2002; Burke 1972; Tuttle et al. 1999) above the Akata Formation. A maximum Agbada Formation thickness of approximately 9000 ft was recorded in the Niger Delta Basin. The Benin Formation is the youngest stratigraphic unit, which becomes thinner toward offshore (Doust and Omatshola 1990) and composed mainly of fluvial sediments (Koledoye and Aydin 2000).

MATERIALS AND METHODS

This work integrates 3D seismic volume, checkshot data, lithological information, geological

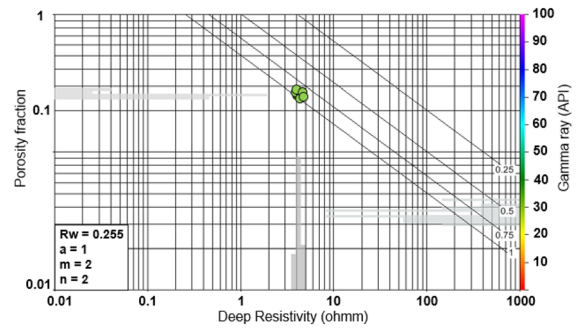


Figure 4. Pickett plot for assessing formation water resistivity (R_w) in the studied wells. Interpreted R_w was used to estimate water saturation (S_w).

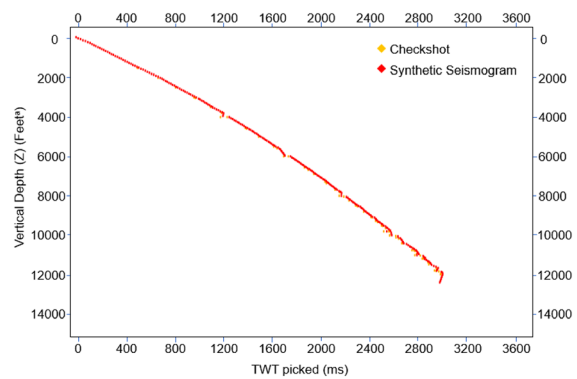


Figure 5. TWT-depth plot using synthetic seismogram and checkshot data of well Q-1 [1 ft = 0.3048 m].

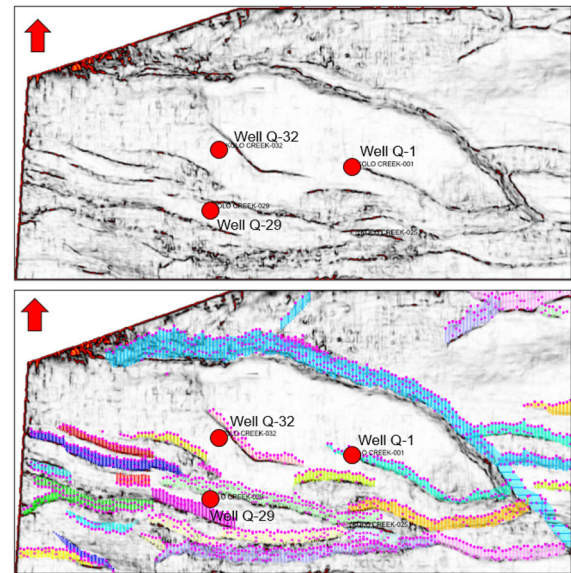


Figure 6. Coherence seismic attribute map at 2256 ms indicating mapped faults and interpreted fault trends.

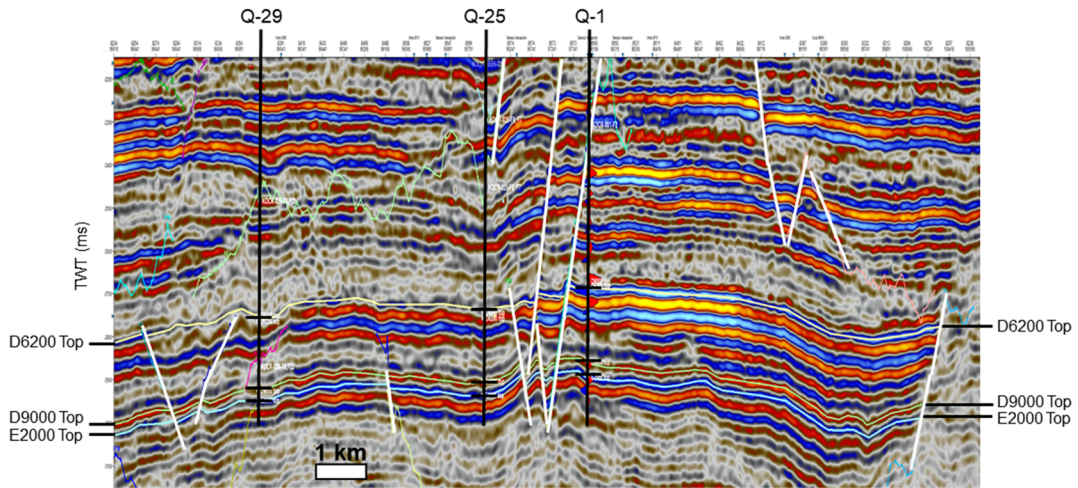


Figure 7. Seismic section showing the correlated reservoir tops (D6200, D9000 and E2000 marked in this section) as confirmed by the well log-based stratigraphic interpretation. Black vertical sticks represent the well locations (Q-29, Q-25 and Q-1).

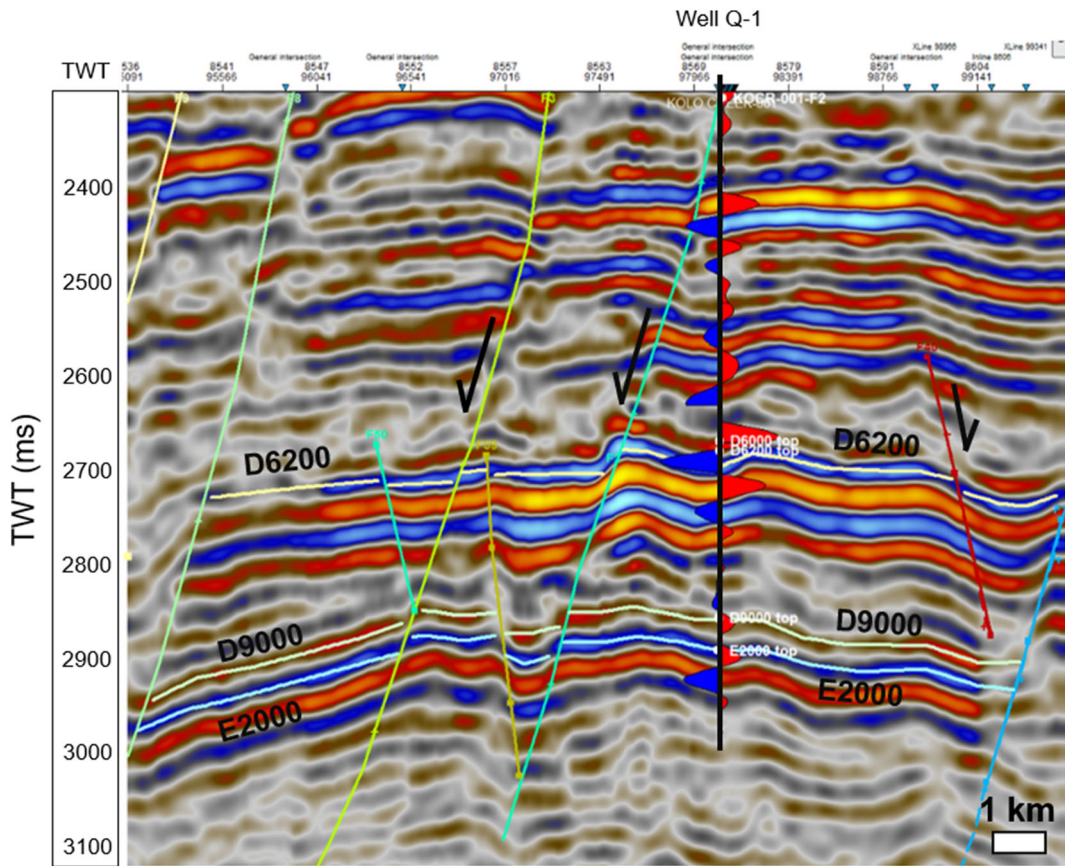


Figure 8. Mapped faults and horizons on traverse line along well Q-1.

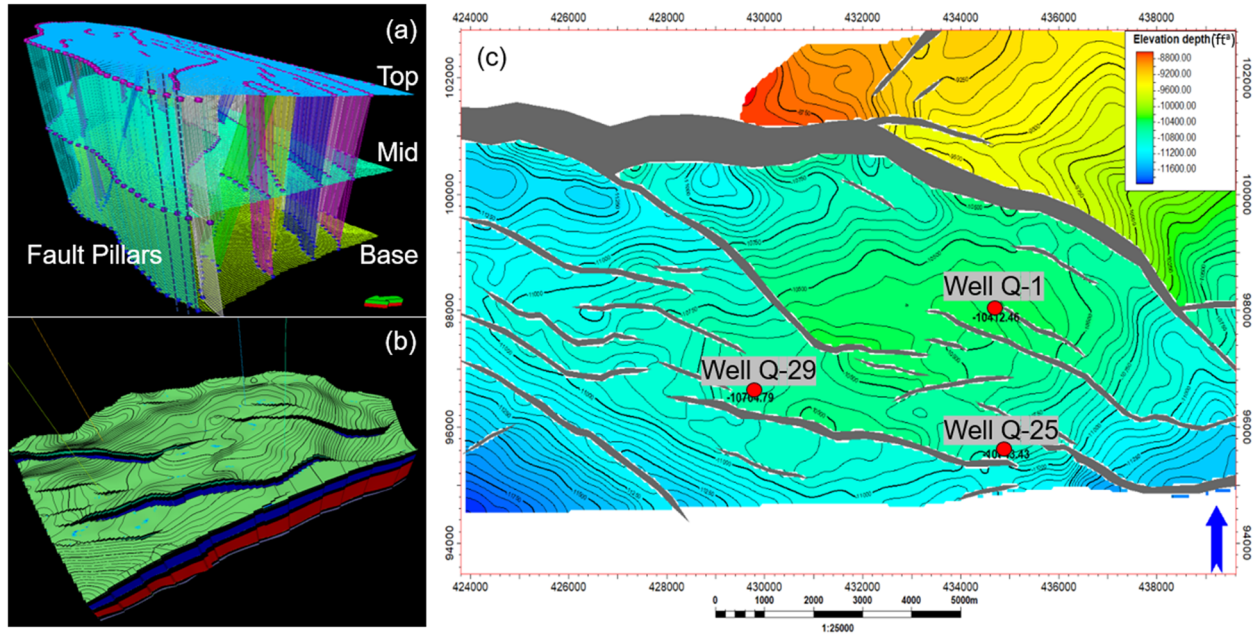


Figure 9. Structural model of the studied Q-Field. **a** Fault pillars as structural framework. **b** Stacked reservoir horizons (D6200–E2000) along with interpreted faults. **c** Depth map at D6200 reservoir top level [^a1 ft = 0.3048 m].

Table 2. Distribution of reservoir intervals in the four studied wells in the Q-Field

Well names	Reservoir intervals (ft) ^a							
	D6200		D7000		D9000		E2000	
	Top	Base	Top	Base	Top	Base	Top	Base
Q-1	10,465	10,620	10,756	10,905	11,304	11,450	11,500	11,709
Q-25	10,818	10,922	11,129	11,202	11,614	11,824	11,772	11,975
Q-29	10,838	10,950	11,150	11,290	11,610	11,720	11,804	11,975
Q-32	10,981	11,110	11,372	11,530	12,137	12,341	12,417	12,630

^a1 ft = 0.3048 m

reports, deviation data and wireline logs (comprising of gamma ray, resistivity, density, neutron porosity and compressional sonic slowness) from drilled wells in the Q-Field. Four wells were available: Q-1, Q-25, Q-29 and Q-32. A well log correlation is presented in Figure 2. Details of the methods and the workflow applied in this work are discussed below.

Seismic Interpretation

A brief summary of the available seismic vintage is presented in Table 1. Seismic data analysis

involved co-ordinate conversion, data loading, well to seismic tie using synthetic seismogram, horizon and fault mapping, time attribute map generation and time to depth conversion (Abdel-Fattah and Alrefaee 2014). Because the well logs are indexed against depth and because seismic data are indexed against time, it was very critical to establish a tie between seismic and well data. This was achieved by using checkshot survey available from the well Q-1 (Fig. 3). Using density (RHOB) and sonic slowness (DT) logs, the acoustic impedance (AI) and reflection coefficients (RC) were generated. RC and Ricker wavelets were then integrated to create a

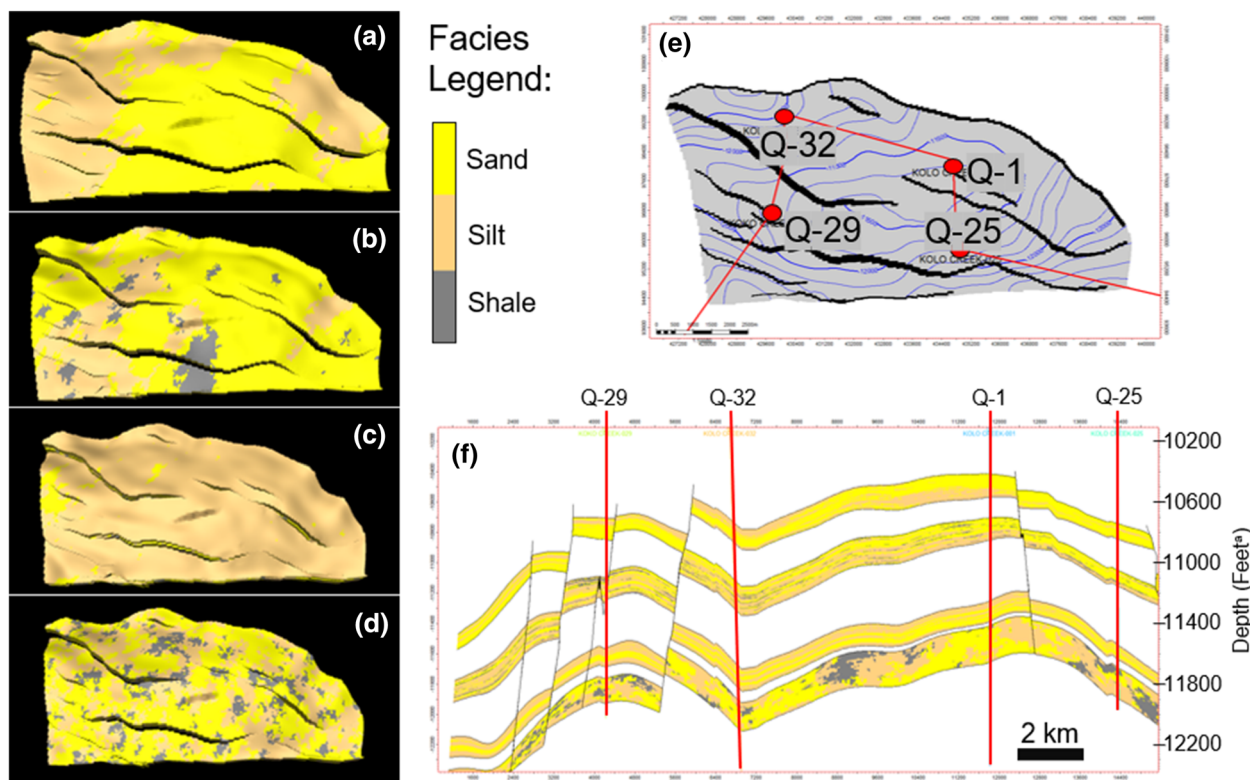


Figure 10. Results of facies modeling in the Q-Field. Left panel presents facies maps at **a** D6200, **b** D7000, **c** D9000 and **d** E2000 reservoir levels. **e** Structural base map and cross-sectional panel line. **f** Facies model in a cross section with the studied well locations [1 ft = 0.3048 m].

synthetic seismogram, which was tied to seismic data by adjusting a bulk shift of 15 ms. After achieving a satisfactory well to seismic tie, as a next step, formation tops from well logs were correlated and marked in the seismic profile together with the structural discontinuities (i.e., faults). Primary seismic reflections corresponding to the top of the main reservoir sands were produced by seismic mapping data (Victor et al. 2019). The selected horizons and faults were later used in 3D reservoir modeling.

Petrophysical Interpretation

Three principal petrophysical parameters were characterized in this work using the wireline logs—porosity, permeability and water saturation. Total porosity (ϕ) was estimated from density log assuming a matrix density value of 2.65 g/cc in the studied clastic intervals. A shale volume correction was applied to assess effective porosity from total porosity. Water saturation (S_w) was estimated by the

Waxman Smits method, and in the absence of produced water analysis, Pickett plot was utilized to evaluate formation water resistivity (R_w), as presented in Figure 4. Permeability was generated using Timur’s equation (Ismail et al. 2020). The standard practice is to validate and calibrate the log-based petrophysical properties with core-based direct measurements. However, in this study, core-based petrophysical properties were unavailable; therefore, all these log-based petrophysical parameters were populated in the 3D static reservoir model to infer the field wide property distribution.

Static Reservoir Modeling

3D geocellular modeling was performed using PETREL software to infer the vertical and horizontal dispositions of the reservoir facies units, structural features and petrophysical properties (Godwill and Waburoko 2016; Abdel-Fattah et al. 2018; Jika et al. 2020). The structural model was

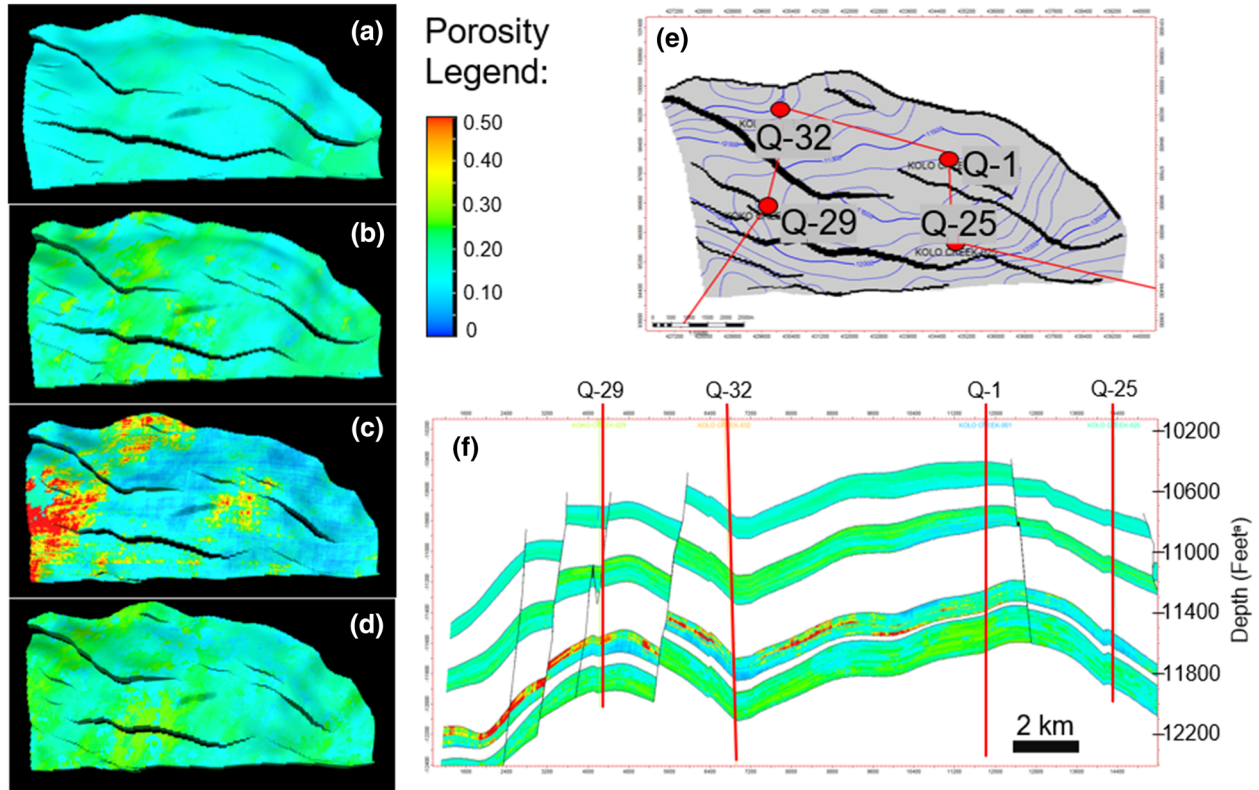


Figure 11. Results of reservoir porosity modeling in the Q-Field. Left panel presents porosity maps at **a** D6200, **b** D7000, **c** D9000 and **d** E2000 reservoir levels. **e** Structural base map and the cross-sectional panel line. **f** Porosity model in a cross section with the studied well locations [^a1 ft = 0.3048 m].

based on the 3D seismic interpretation. The input data consisted of reservoir surface tops, polygons and measured fault surfaces. The first phase in developing a field structural model was to select the horizons and mark the fault based on the vertical dispositions of the correlated horizons. A 3D grid divides the space into cells in which materials are considered to be almost identical (Edwin et al. 2011; Olubunmi and Olawale 2018). Depending on the definition, the defects were mainly modeled on the input fault surfaces (Adeoti et al. 2014). The structural skeleton consisted of top, mid and base grid levels, where 3D fault pillars were interpreted after sealing the fault connections with the horizons (Haque et al. 2016) and then utilized to generate consecutive structural maps at various target formation top levels.

In view of the definition of the reservoir, the areal dimensions of the grid cells were set at 50 ft by 50 ft. There were $252 \times 125 \times 65$ cells in the 3D static model. Once the seismic-based structural modeling was achieved, a velocity model was constructed to convert the structural domain from time

domain to depth domain before running facies and petrophysical modeling (Abdel-Fattah and Tawfik 2015; Abdel-Fattah et al. 2015, 2018). Simulation of Sequential Indicator (SIS) technology was used for facies modeling in 3D space by a stochastic approach (Journel 1982; Deutsch and Journel 1998; Remy et al. 2009) (see “Appendix”). The approach allows for simple modeling of facies where vertically, laterally or, otherwise, the volumes of facies vary. The wells were labeled on the basis of the log data available (mostly gamma ray log) in facies associations. A gamma ray cutoff of $GR > 75$ API was used to distinguish the non-reservoir facies. The facies realizations were conditioned to the wells during the facies modeling phase, and several realizations were performed in the facies modeling to catch the intrinsic heterogeneity, if any. Well-based petrophysical interpretations were up-scaled and stochastically distributed using Sequential Gaussian Simulation (SGS) method (Maleki Tehrani et al. 2012; Geboy et al. 2013) within the respective facies distributions in 3D space (see “Appendix”).

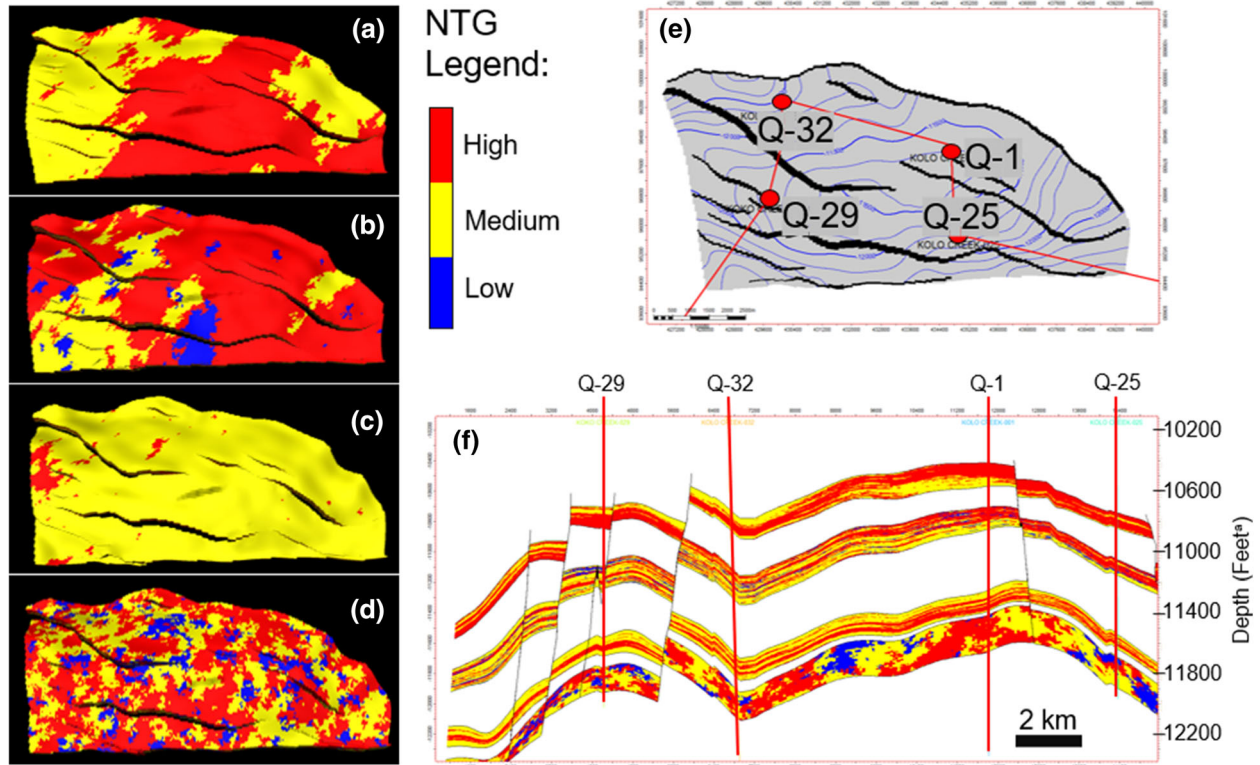


Figure 12. Results of net-to-gross (NTG) modeling in the Q-Field. Left panel presents NTG maps at **a** D6200, **b** D7000, **c** D9000 and **d** E2000 reservoir levels. **e** Structural base map and the cross-sectional panel line. **f** NTG model in a cross section with the studied well locations [^a1 ft = 0.3048 m].

Volumetric Analysis

Reservoir volumetric is the mechanism by which the hydrocarbon concentration in a reservoir is determined (Ali et al. 2020; Egbe et al. 2019). It is really important because it serves as a reference for exploring and developing fields. After a static field model was created, the structural model and the constructed petrophysical model were used to measure the reserves in terms of stock tank of original oil in place (STOOIP) and gas initially in place (GIIP) of the reservoir under study using the following equations:

$$STOIP(STB) = 7758Ah\phi(1 - S_w) \frac{1}{B_o} \quad (1)$$

$$GIIP = \left(\frac{43,560Ah\phi(1 - S_w)}{B_{gi}} \right) \quad (2)$$

where *A* is area in acres, *h* is net pay thickness in feet, ϕ is porosity, *S_w* is water saturation, *B_o* is for-

mation volume factor, and *B_{gi}* is gas formation volume factor.

RESULTS AND DISCUSSION

In the studied Q-Field, a confident well to seismic tie was achieved using the checkshot data of well Q-1, which provided great compatibility (Fig. 5). A seismic coherence attribute map (Fig. 6) provided critical information in identification of several faults and their extension. Faults and horizons were mapped in the seismic volume, guided by the well log-based interpretations (Figs. 7 and 8). Based on the horizon and fault mapping in the seismic volume, fault pillars were interpreted and structural modeling was performed (Fig. 9). Time and depth structure maps display network of development faults, which stretched up to 80% of the mapped area’s whole breath. Series of normal faults dominated the whole mapped area, catego-

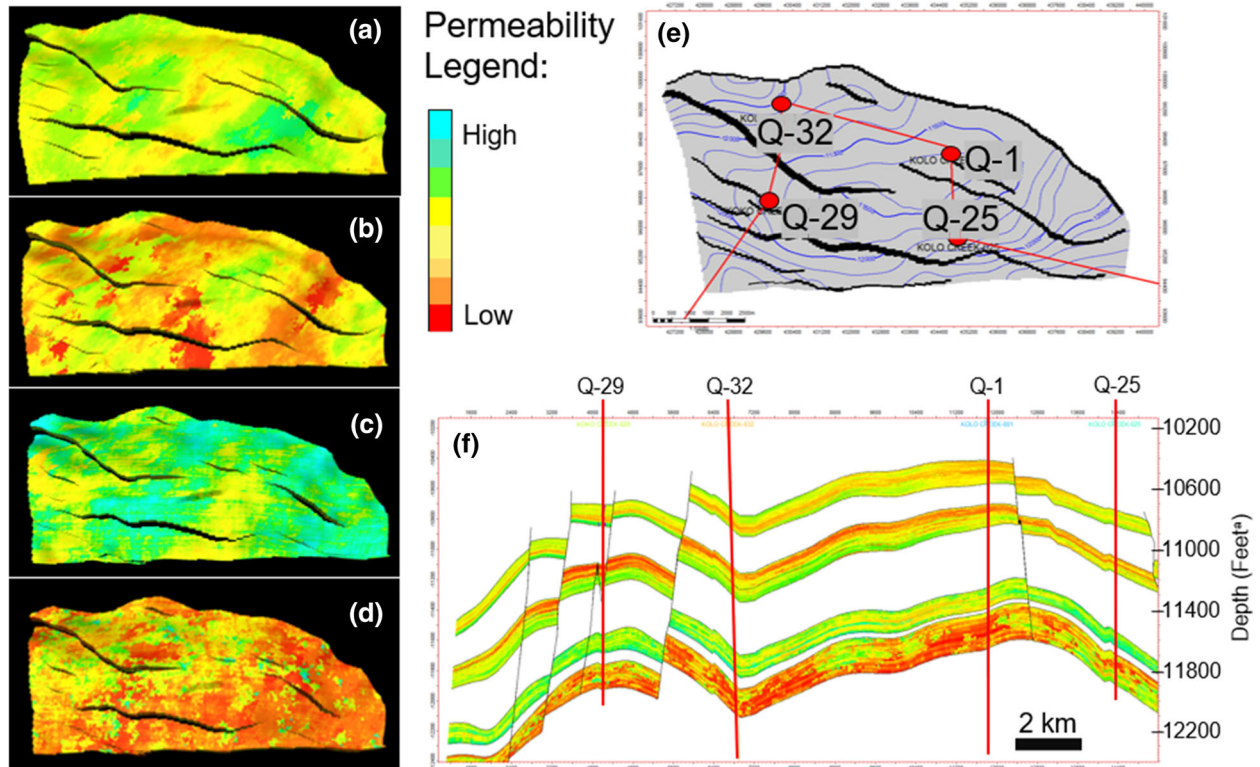


Figure 13. Results of permeability modeling in the Q-Field. Left panel presents permeability maps at **a** D6200, **b** D7000, **c** D9000 and **d** E2000 reservoir levels. **e** Structural base map and the cross-sectional panel line. **f** Permeability model in a cross section with the studied well locations [$1 \text{ ft} = 0.3048 \text{ m}$].

rized as syn-depositional listric faults and minor antithetic faults. Principal normal faults were NW–SE trending and dipped toward SW. These faults assisted in hydrocarbon trapping mechanism in the Q-Field.

Petrophysical investigation identified four principal reservoir intervals; these are D6200, D7000, D9000 and E2000 from shallow to deep. Both the well logs and seismic horizon mapping indicated that these reservoirs are laterally extensive throughout the modeled area and affected by the interpreted normal faults. Reservoir interval distributions in the studied wells are documented in Table 2. Average porosity and permeability in these reservoirs vary in the range of 17.9–21.6% and 62–105 mD, respectively. Reservoir net-to-gross (NTG) varies in the range of 0.6–1. Water saturation varies from 36.3 to 74%, while hydrocarbon saturation values vary in the range from 26 to 63.7%. The 3D static reservoir modeling was performed to infer the lateral and vertical distributions of the facies assemblage (Fig. 10), porosity (Fig. 11), NTG

(Fig. 12), permeability (Fig. 13) and water saturation (Fig. 14) throughout the Q-Field.

In general, the 3D facies model depicted larger probability distribution of sand (dominantly) and minor silts in all the reservoirs (Fig. 10), although the D9000 reservoir was mostly silty and E2000 was, lithologically, more heterogeneous in both vertical and lateral scales. The top reservoir D6200 had an average thickness range of 104–155 ft, as encountered in the four wells. The facies model indicated a dominance of sands with minor silt distribution in the D6200 reservoir, which translated into high NTG value and a more homogenous porosity–permeability distribution. The static modeling results showed that the D7000 reservoir properties were very similar to that of the D6200 interval in terms of major facies distribution, porosity and NTG distribution; however, it had lower permeability and higher water saturation than the overlying reservoir. D9000 reservoir was dominated by silty facies distribution, resulting in lesser porosity and moderate to poor NTG. In the western part of the Q-Field, the D9000

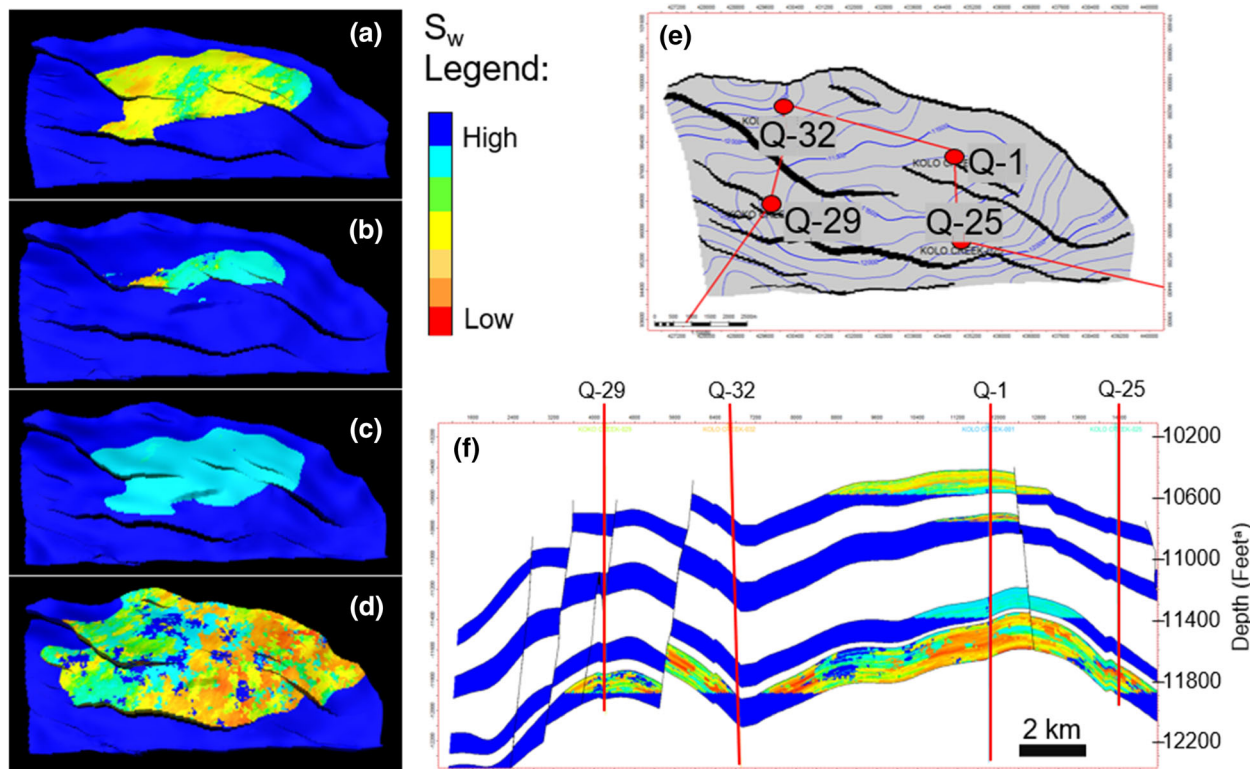


Figure 14. Results of water saturation (S_w) modeling in the Q-Field. Left panel presents S_w maps at **a** D6200, **b** D7000, **c** D9000 and **d** E2000 reservoir levels. **e** Structural base map and the cross-sectional panel line. **f** S_w model in a cross section with the studied well locations [^a1 ft = 0.3048 m].

reservoir showed higher abundance of sand facies comprising of higher porosity and NTG. The bottom most reservoir E2000 provided the maximum reservoir thickness of 171–213 ft, and it was found to be heterogeneous in terms of reservoir properties. Sand facies was less laterally extensive, rather discontinuous when compared to the upper reservoirs, resulting in a wide NTG distribution throughout, greater variability of water saturation and lower permeability in the E2000 reservoir interval.

The dominant reservoir fluid type is gas. Out of the four studied wells, only Q-1, being drilled in the anticline, had encountered hydrocarbon columns in all the reservoirs, while Q-32 was drilled in the synclinal position and passed through the reservoir water legs. The Q-25 and Q-29 encountered both gas and oil only in the E2000 reservoirs. The lateral and vertical distributions of the interpreted hydrocarbons were populated through the static reservoir modeling (Fig. 15). Gas-down-to exists in the upper three reservoirs (D6200, D7000 and D9000) of the well Q-1 at 10,577 ft, 10,756 ft and 11,389 ft, respectively. Gas–oil and oil–water contacts were

interpreted in the deepest reservoir interval E2000 at 11,812 ft and 11,886 ft, respectively. The interpreted fluid contact depths and reservoir volumetrics (gas and oil in place) of the studied reservoirs are presented in Table 3.

CONCLUSIONS

The present 3D static reservoir modeling work presents a clearer understanding of the field-wide distribution of the reservoir facies, structural style and petrophysical parameters in the Q-Field, Niger Delta, Nigeria. Four clastic Eocene reservoir intervals (D6200, D7000, D9000 and E2000) were studied using four wells drilled across the Q-Field. Normal faults with NW–SE trends, which acted as hydrocarbon traps in the study area, were interpreted from the seismic data and 3D structural modeling. Facies modeling indicated extensive lateral continuity of the sand-dominated reservoir facies. Overall, a narrow porosity range of 18–22% was found from the 3D reservoir petrophysical modeling. The

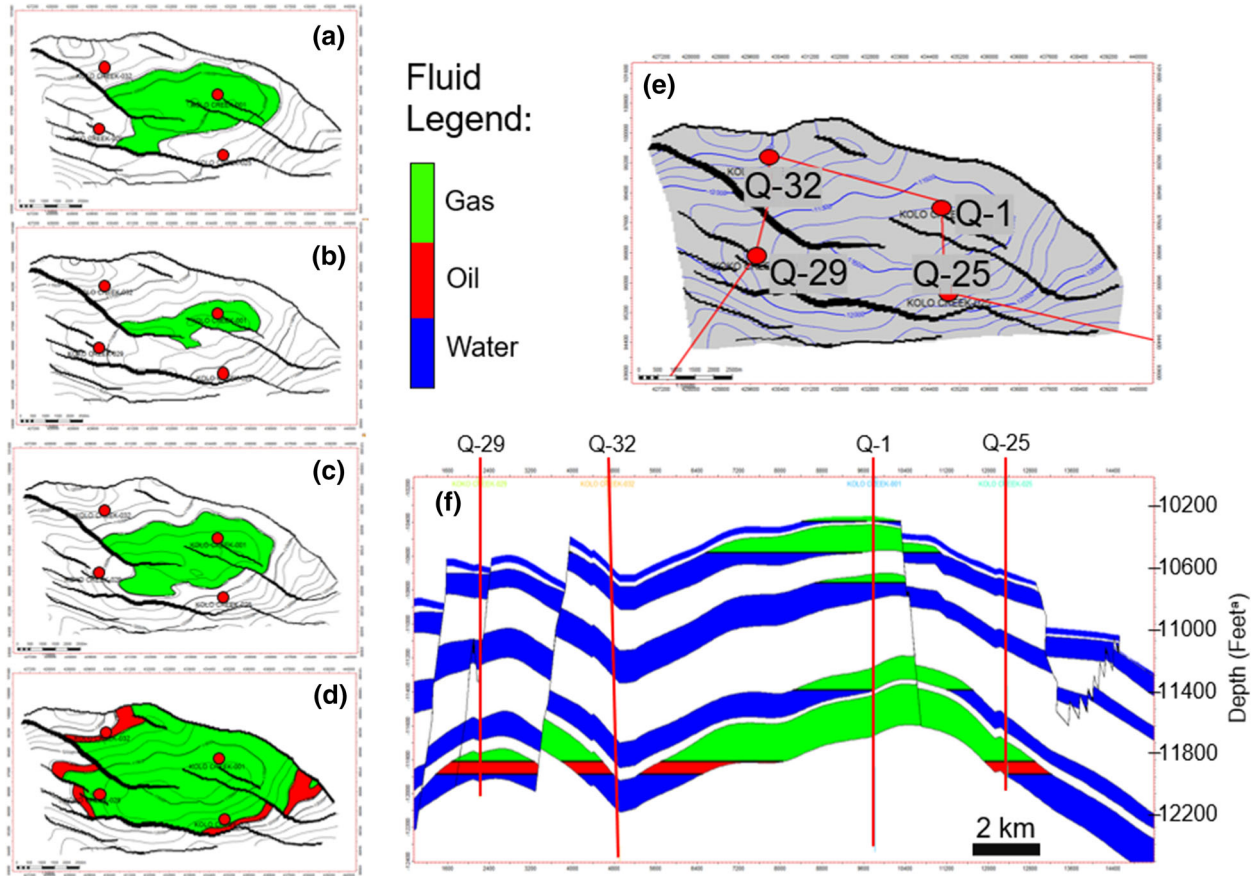


Figure 15. Results of hydrocarbon distribution modeling in the Q-Field. Left panel presents hydrocarbon extension maps at **a** D6200, **b** D7000, **c** D9000 and **d** E2000 reservoir levels. **e** Structural base map and the cross-sectional panel line. **f** Gas–oil–water distribution and fluid contacts in a cross section with the studied well locations [^a1 ft = 0.3048 m].

Table 3. Hydrocarbon contacts, average porosity, water saturation, and hydrocarbon volume estimates in the four studied reservoir intervals of the Q-Field

Reservoir intervals	Fluid contacts (ft) ^a			Average porosity (%)	Average water saturation (%)	GIIP (BSCF) ^b	STOIIP (MMSTB) ^c
	GDT	GOC	OWC				
D6200	10,577	–	–	17.9	36.3	4930.16	–
D7000	10,756	–	–	21.6	52.2	647.06	–
D9000	11,389	–	–	18.4	74	1495.35	–
E2000	–	11,812	11,886	20.4	38	21,349.95	115.05

GDT gas-down-to, *GOC* gas–oil contact, *OWC* oil–water contact, *GIIP* gas initially in place in billions of standard cubic feet (BSCF)^b unit, *STOIIP* stock tank of original oil in place in million stock tank barrels (MMSTB)^c unit

^a1 ft = 0.3048 m

^b1 ft³ = 0.0283 m³

^c1 barrel = 0.0158 m³

reservoirs exhibited medium to high NTG and heterogeneous permeability distribution across the four reservoir levels. Water saturation modeling and fluid distribution maps indicated that the hydrocar-

bon accumulation was restricted in the structural highs, i.e., anticlines, in the central part of the Q-Field, as confirmed by fluid contacts in three studied wells (Q-1, Q-25 and Q-29). The subsurface geo-

logical model, presented in this work, will be critical for a further development program of the reservoirs. It will help to better identify future well locations. Future work will involve further detailing and fine-tuning of the reservoir models based on future well data.

ACKNOWLEDGMENT

We are grateful to John Carranza, Ph.D., Editor-in-Chief, Natural Resources Research and to the two reviewers for their critical suggestions and constructive reviews which benefited this manuscript. Authors acknowledge SPDC Nigeria for providing the data set. The authors extend their sincere appreciation to the Researchers Supporting Project number (RSP-2020/92), King Saud University, Riyadh, Saudi Arabia.

APPENDIX

Sequential Indicator Simulation (SIS)

SIS is used for a discrete or categorical variable. The algorithm for SIS depends on indicator kriging to infer the cumulative distribution function (CDF) of a discrete variable $Z(u)$. It simulates in cases where data are not required to fit a normal distribution with the sequential paradigm (Remy et al. 2009). Through stochastic simulation, equally probable realizations of the distribution of an indicator variable are produced (Journel 1982; Deutsch and Journel 1998). The steps in SIS are as follows.

- (i) Select pixels where the lithotype is unknown.
- (ii) Identify neighboring node points with known lithotypes.
- (iii) Assign weights to the neighboring points.
- (iv) Construct a local (CDF) for lithotype probability from the neighbor lithotypes.
- (v) Extraction forms the CDF of a single lithotype to occupy the empty node points.
- (vi) Random selection of another empty node point.
- (vii) Proceed to Step 1 and repeat until estimations have been made at all the empty node points.

Sequential Gaussian Simulation (SGS)

SGS is a stochastic modeling technique that obtains multiple realizations based on the same input data (Maleki Tehrani et al. 2012; Geboy et al. 2013). The steps of SGS consist of the following.

- (i) Select a node point where the reservoir property under investigation is unknown.
- (ii) Recognize adjacent node points where the property is known.
- (iii) Then, allocate weights to the neighbors, depending on their observed relevance at empty node points.
- (iv) Construct a local probability distribution function (pdf) at the empty node points from the neighbor values.
- (v) Extraction forms the pdf of a single value to occupy the empty node points, a random selection of another empty node points.
- (vi) Proceed to Step 1 and repeat until estimations have been made at all empty node points.

REFERENCES

- Abdel-Fattah, M., & Alrefae, H. (2014). Diacritical seismic signatures for complex geological structures: Case studies from Shushan Basin (Egypt) and Arkoma Basin (USA). *International Journal of Geophysics*. <https://doi.org/10.1155/2014/876180>.
- Abdel-Fattah, M., Dominik, W., Shendi, E., Gadallah, M., & Rashed, M. (2010). 3D integrated reservoir modelling for Upper Safa Gas Development in Obaiyed Field, Western Desert, Egypt. In *72nd EAGE Conference and Exhibition Incorporating SPE EUROPEC*, Spain, June 2010. <https://doi.org/10.3997/2214-4609.201401358>.
- Abdel-Fattah, M., Gameel, M., Awad, S., & Ismaila, A. (2015). Seismic interpretation of the Aptian Alamein dolomite in the Razzak oil field, Western Desert, Egypt. *Arabian Journal of Geosciences*, 8(7), 4669–4684.
- Abdel-Fattah, M. I., Metwalli, F. I., & El Sayed, I. M. (2018). Static reservoir modeling of the Bahariya reservoirs for the oilfields development in South Umbarka area, Western Desert, Egypt. *Journal of African Earth Sciences*, 138, 1–13.
- Abdel-Fattah, M. I., & Tawfik, A. Y. (2015). 3D geometric modeling of the Abu Madi reservoirs and its implication on the gas development in Baltim area (Offshore Nile Delta, Egypt). *International Journal of Geophysics*. <https://doi.org/10.1155/2015/369143>.
- Adagunodo, T. A., Sunmonu, L. A., Adabanija, M. A., Oladejo, O. P., & Adenji, A. A. (2017). Analysis of fault zones for reservoir modeling in Taa field, Niger Delta, Nigeria. *Petroleum and Coal*, 59(3), 378–388.
- Adelu, A. O., Aderemi, A. A., Akanij, A. O., Sanuade, O. A., Kaka, S. I., Afolabi, O., et al. (2019). Application of 3D static

- modeling for optimal reservoir characterization. *Journal of African Earth Sciences*, 152, 184–196.
- Adeoti, L., Onyekachi, N., Olatinsu, O., Fatoba, J., & Bello, M. (2014). Static reservoir modeling using well log and 3-D seismic data in a KN Field, Offshore Niger Delta, Nigeria. *International Journal of Geosciences*, 5, 93–106.
- Adesoji, O. A., Oluseun, A. S., SanLinn, I. K., & Isaac, D. B. (2018). Integration of 3D seismic and well log data for the exploration of Kini Field, Offshore Niger Delta. *Petroleum and Coal*, 60(4), 752–761.
- Adiela, U. P. (2018). Reservoir modeling using seismic attributes and well log analysis: A Case study of Niger Delta, Nigeria. In: *AAPG International Conference and Exhibition, Cape Town, South Africa, Nov 4–11*. AAPG Search and Discovery Article # 90332.
- Agbasi, O. E., Igboekwe, M. U., Chukwu, G. U., & Sunday, E. E. (2018). Discrimination of pore fluid and lithology of a well in X Field, Niger Delta, Nigeria. *Arabian Journal of Geosciences*, 11, 274. <https://doi.org/10.1007/s12517-018-3610-7>.
- Agbasi, O. E., Sen, S., Inyang, N. J., & Etuk, S. E. (2020). Assessment of pore pressure, wellbore failure and reservoir stability in the Gabo field, Niger Delta, Nigeria-implications for drilling and reservoir management. *Journal of African Earth Sciences*, 173, 104038.
- Ahmed, H., Nyeche, M., Engel, S., Nworie, E., & De Mooij, H. (2011). 3D reservoir simulation of X field onshore Niger Delta, Nigeria: The power of multiple iterations. In: *SPE Nigeria International Conference and Exhibition, Abuja, Nigeria, July 30–Aug 3*. SPE-150730-MS. <https://doi.org/10.2118/150730-MS>.
- Aigbadon, G. O., Okoro, A. U., Una, C. O., & Ocheli, A. (2017). Depositional facies model and reservoir characterization of USANI field 1, Niger Delta Basin, Nigeria. *International Journal of Advanced Geosciences*, 5(2), 57–68.
- Alao, P. A., Olabode, S. O., & Opeloye, S. A. (2013). Integration of seismic and petrophysics to characterize reservoirs in “ALA” Oil Field, Niger Delta. *The Scientific World Journal*. <https://doi.org/10.1155/2013/421720>.
- Ali, M., Abdelhady, A., Abdelmaksoud, A., Darwish, M., & Essa, M. A. (2020). 3D Static modeling and petrographic aspects of the Albian/Cenomanian Reservoir, Komombo Basin, Upper Egypt. *Natural Resources Research*, 29, 1259–1281.
- Burke, K. (1972). Longshore drift, submarine canyons, and submarine fans in development of Niger Delta. *American Association of Petroleum Geologists*, 56, 1975–1983.
- Deutsch, C. V., & Journel, A. G. (1998). *Geostatistical software library (GSLIB)* (2nd ed., p. 369). Oxford: Oxford University Press.
- Doust, H., & Omatsola, E. (1990). Niger Delta. In: Edwards, J.D., Santogrossi, P.A. (eds.) *Divergent/passive margin basins* (vol. 48, pp. 239–248). AAPG Memoir.
- Edwin, E. V., Jose, L. P., Carlos, A. M., & María, C. H. (2011). High resolution stratigraphic controls on rock properties distribution and fluid flow pathways in reservoir rocks of the Upper Caballos Formation, San Francisco Field, Upper Magdalena Valley, Colombia. In *South American Oil and Gas Congress, SPE Western Venezuela Section, Maracaibo, Venezuela, Oct 18–21*. SPE WVS 095.
- Egbe, T., Ugwu, S. A., & Ideozu, R. U. (2019). Reservoir characterization of Buma Field Reservoirs, Niger Delta using Seismic and Well Log Data. *Petroleum and Chemical Industry International*, 2(4), 1–11.
- Ejedavwe, J., Fatumbi, A., Ladipo, K., & Stone, K. (2002). Pan—Nigeria exploration well look—back (Post-Drill Well Analysis). Shell Petroleum Development Company of Nigeria Exploration Report 2002.
- Farouk, I. M., El-Arabi, H. S., & Mohamed, S. F. (2017). Reservoir petrophysical modeling and risk analysis in reserve estimation: A Case Study from Qasr Field, North Western Desert, Egypt. *Journal of Applied Geology and Geophysics (IOSR-JAGG)*, 5(2), 41–52.
- Geboy, N. J., Olea, R. A., Engle, M. A., & Martín-Fernández, J. A. (2013). Using simulated maps to interpret the geochemistry, formation and quality of the blue gem coal bed, Kentucky, USA. *International Journal of Coal Geology*, 112, 26–35.
- Godwill, P. A., & Waburoko, J. (2016). Application of 3D reservoir modeling on Zao 21 Oil Block of Zilaitun Oil Field. *Journal of Petroleum Environmental and Biotechnology*, 7, 262. <https://doi.org/10.4172/2157-7463.1000262>.
- Haque, A. K. M. E., Islam, M. A., & Shalaby, M. R. (2016). Structural modeling of the Maui Gas Field, Taranaki Basin, New Zealand. *Petroleum Exploration Development*, 43(6), 883–892.
- Inyang, N. J., Akpabio, O. I., & Agbasi, O. E. (2018). Shale volume and permeability of the Miocene unconsolidated Turbidite sand of Bonga Oil Field, Niger Delta, Nigeria. *International Journal of Advanced Geoscience*, 5(1), 37–45.
- Ismail, A., Raza, A., Gholami, R., & Reza, R. (2020). Reservoir characterization for sweet spot detection using color transformation overlay scheme. *Journal of Petroleum Exploration and Production Technology*, 10, 2313–2334.
- Jika, H. T., Onuoha, K. M., & Dim, C. I. P. (2019). Application of geostatistics in facies modeling of Reservoir-E, “Hatch Field” offshore Niger Delta Basin, Nigeria. *Journal of Petroleum Exploration and Production Technology*, 10, 769–781.
- Jika, H. T., Onuoha, M. K., Okeugo, C. G., & Eze, M. O. (2020). Application of sequential indicator simulation, sequential Gaussian simulation and flow zone indicator in reservoir-E modelling; Hatch Field Niger Delta Basin, Nigeria. *Arabian Journal of Geosciences*, 13, 410.
- Journel, A. (1982). The indicator approach to estimation of spatial distributions. In *17th APCOM Symposium Proceedings. Society of Mining Engineers* (pp. 793–806).
- Kalu, C. G., Obiadi, I. I., Amaechi, P. O., & Ndeze, C. K. (2020). petrophysical analysis and reservoir characterization of emerald field, Niger Delta Basin, Nigeria. *Asian Journal of Earth Sciences*, 13, 21–36.
- Koledoye, A. B., & Aydin, A. A. (2000). Three-dimensional visualization of normal faults segmentation and its implication for faults growth. *The Leading Edge*, 19(7), 692.
- Ma, Y. Z., & Pointe, P. L. (2011). Uncertainty analysis and reservoir modeling: Developing and managing assets in an uncertain world. In: Y. Z. Ma & P. L. Pointe (Eds.), *AAPG Memoir* (vol. 96).
- Maleki Tehrani, M. A., Asghari, O., & Emery, X. (2012). Simulation of mineral grades and classification of mineral resources by using hard and soft conditioning data: application to Sungun porphyry copper deposit. *Arabian Journal of Geosciences*, 6, 3773–3781.
- Ndip, E. A., Agyingyi, C. M., Nton, M. E., & Oladunjoye, M. A. (2018). Seismic stratigraphic and petrophysical characterization of reservoirs of the Agbada Formation in the Vicinity of ‘Well M’, Offshore Eastern Niger Delta Basin, Nigeria. *Journal of Geology and Geophysics*, 7, 331. <https://doi.org/10.4172/2381-8719.1000331>.
- Okpogo, E. U., Abbey, C. P., & Atueyi, I. O. (2018). Reservoir characterization and volumetric estimation of Orok Field, Niger Delta hydrocarbon province. *Egyptian Journal of Petroleum*, 27(4), 1087–1094.
- Olubunmi, C. A., & Olawale, O. A. (2018). Structural interpretation, trapping styles and hydrocarbon potential of Block-X, Northern Depobelt, Onshore Niger Delta. In: *AAPG Annual Convention and Exhibition, Salt Lake City, Utah, May 20–23*. AAPG Search and Discovery Article # 11099.
- Oluwadare, O. A., Osunrinde, O. T., Abe, S. J., & Ojo, B. T. (2017). 3-D geostatistical model and volumetric estimation of

- 'Del' Field, Niger Delta. *Journal of Geology and Geophysics*, 6, 291. <https://doi.org/10.4172/2381-8719.1000291>.
- Omoja, U. C., & Obiekezie, T. N. (2018). Application of 3D seismic attribute analyses for hydrocarbon prospectivity in Uzot-Field, Onshore Niger Delta Basin, Nigeria. *International Journal of Geophysics*. <https://doi.org/10.1155/2019/1706416>.
- Oyeyemi, K. D., Olowokere, M. T., & Aizebeokhai, A. P. (2018). Hydrocarbon resource evaluation using combined petrophysical analysis and seismically derived reservoir characterization, offshore Niger Delta. *Journal of Petroleum Exploration and Production Technology*, 8, 99–115.
- Remy, N., Boucher, A., & Wu, J. B. (2009). *Applied geostatistics with SGeMS* (p. 264). Cambridge: Cambridge University Press.
- Seyyedattar, M., Zendehbiudi, S., & Butt, S. (2020). Technical and non-technical challenges of development of offshore petroleum reservoirs: Characterization and production. *Natural Resources Research*, 29, 2147–2189.
- Tuttle, M. L., Charpentier, R. R., & Brownfield, M. E. (1999). The Niger Delta petroleum system; Niger Delta Province, Nigeria, Cameroon, and Equatorial Guinea, Africa. *United States Geological Survey (USGS) Open-File Report 99-50-H*. <https://doi.org/10.3133/ofr9950H>.
- Victor, C. N., Kingsley, C. E., & Tuoyo, A. E. (2019). Evaluation of hydrocarbon reserves using integrated petrophysical analysis and seismic interpretation: A case study of TIM field at southwestern offshore Niger Delta oil Province, Nigeria. *Egyptian Journal of Petroleum*, 28(3), 273–280.
- Yu, X. Y., Ma, Y. Z., Psaila, D., Pointe, P. L., Gomez, E., & Li, S. (2011). Reservoir characterization and modeling. In Y. Z. Ma & P. LaPointe (Eds.), *Uncertainty analysis and reservoir modeling. A look back to see forward* (vol. 96, pp. 289–309). AAPG Memoir.